BIPARAMETRIC CLUTTER-MAP CFAR PROCESSOR INDEPENDENT OF ORIGINAL CLUTTER DISTRIBUTION

Yan Lin, Jun Tang, Xiutan Wang, Huadong Meng

Department of Electronic Engineering, Tsinghua University, Beijing 100084, China

ABSTRACT

The traditional CFAR processors are based on the sliding-window concept, which have substantial performance degradation under nonhomogeneity. Owing to temporal processing and the exploitation of the local homogeneity of the map cell, the clutter-map procedure acquires enhanced robustness with little CFAR losses. In this paper, a Gaussian biparametric clutter-map constant false alarm rate (GBCM-CFAR) processor is proposed which merges the clutter-map technique and noncoherent integration together. It can approximately achieve CFAR independent of the original clutter distribution. The performance in the presence of fast point targets is assessed, in the examples of Weibull and lognormal clutter, in order to elicit the effect of the system parameters. Its performance is close to that of the optimum Neyman-Pearson detector with little CFAR losses in homogeneous environments. It is also suitable to deal with the nonhomogeneous situation.

1. INTRODUCTION

Constant false alarm rate (CFAR) processors are widely used in radar detection to achieve control of the false alarm rate under varying environments. Most of the proposed CFAR systems accomplish estimation of the background level by processing a bunch of samples, which represent the clutter echoes from the spatial cells in close proximity to the test cell. The estimation sample coincides with a finite size window, thus these systems are referred as sliding-window CFAR (SW-CFAR). The SW-CFAR processor can achieve good performance in homogeneous or near homogeneous environments. However, its performance may severely degrade due to non-homogeneities, which lead to abrupt variations in the statistical properties of the echoes across the reference cells [1].

The clutter-map CFAR (CM-CFAR) [2] detector relies on another concept, where the radar space is divided into several map cells, each containing one or more spatial cells. In each scan, the background level estimation of each map cell is updated by digital exponential smoothing of the clutter returns, memory stored and used in next scan. The CM-CFAR processor will not suffer from non-homogeneities, provided that the size of the map cell is small enough. But it suffers the masking effect, which leads to the performance degradation due to targets dwelling in the same map cell for several scans.

Previous studies on the CM-CFAR detector have been limited to a single pulse. In this paper, we extend the analysis of the CM-CFAR detector with R-pulse noncoherent integration to get the explicit formulas of the false alarm rate and the detection probability. The CFAR property of such processor is proven by using an ancillary statistic with some approximations. We call this processor Gaussian biparametric clutter-map CFAR (GBCM-CFAR). Based on the fact that the result of noncoherent integration of the amplitudes of independent clutter samples is approximately identical to a Gaussian distribution, provided that the integration number is large enough, it can approximately achieve CFAR independent of original clutter distribution. This property is the same as the Gaussian biparametric CFAR (GB-CFAR) [3] that is based on the sliding-window concept. But GBCM-CFAR is more suitable to the real situation than GB-CFAR (or SW-CFAR) to cope with nonhomogeneities. Since GBCM-CFAR relies on updating the background estimate corresponding to the map cell scan-by-scan, the map cell size turns out to be much smaller than that of the reference window of GB-CFAR (or SW-CFAR). The performance of the GBCM-CFAR detector with regard to Weibull and lognormal clutter is analyzed. We shall show that its performance under homogeneity is close to the optimal.

2. ANALYSIS OF THE GBCM-CFAR DETECTOR

The GBCM-CFAR detector is shown in Fig. 1. Following linear-law detection and R-pulse noncoherent integration, the integrated data of M spatial cells belonging to the map cell being scanned are fed to the mean estimator and the variance estimator to get the sample mean $\overline{X}(n)$ and the sample variance $S^2(n)$ of the n th scan. Then the sample mean and the sample variance undergo digital exponential smoothing by two single-pole loop integrators to update the two estimates for the next scan. The loop integrator with feedback gain a is outlined in Fig. 2. It supplies an asymptotically unbiased estimate of the expected value of

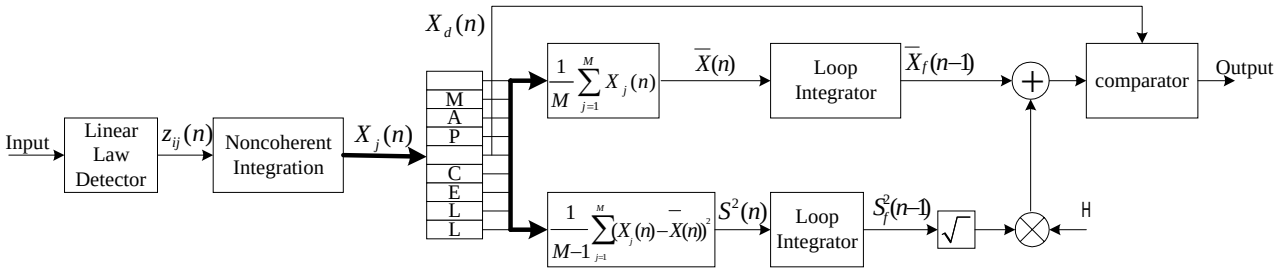

Figure 1: Block scheme of the GBCM-CFAR processor

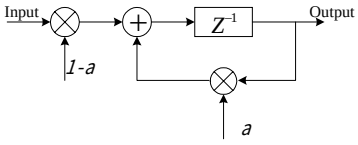

Figure 2: Loop integrator

its input. The smoothed sample mean plus the product of the smoothed sample standard deviation and a fixed coefficient H forms the threshold. The integrated value of the test cell is not compared with the current threshold value, but with the value stored in the previous scan, so as to avoid useful targets returns causing overestimation of the threshold. Let $\overline{X}_f(n-1)$ denote the output of the upper integrator, $S_f^2(n-1)$ denote the output of the lower integrator at the $(n-1)$ th scan. The value of the test cell is presented as $X_d(n)$. Hence the detection decision at the n th scan is made as following:

$$X_d(n) \underset{H_0}{\overset{H_1}{\gtrless}} \overline{X}_f(n-1) + H\sqrt{S_f^2(n-1)} \qquad (1)$$

In the following, we refer to the situation that the environment is clutter dominated, namely that the thermal noise component can be neglected. It is assumed that the amplitudes of the returns from the spatial cells in the same map cell are independent and identically distributed (i.i.d.) and uncorrelated on a scan-by-scan basis, i.e. that the radar carrier frequency varies at least scan-by-scan. Let the amplitudes of the spatial cells belonging to the map cell at n th scan denote by $z_{ij}(n)$ $(1 \le i \le R, 1 \le j \le M)$. Performing noncoherent integration generates the new statistic:

$$X_j(n) = \sum_{i=1}^{R} z_{ij}(n) \qquad (2)$$

$X_j(n)$ is approximately identical to Gaussian distribution when the integration number is large enough [4], i.e. $X_j(n) \sim N(m_R, \sigma_R^2)$, where m_R, σ_R^2 denote the mean and the variance of the amplitudes after integration respectively. And $m_R = Rm_z$, $\sigma_R^2 = R\sigma_z^2$, where m_z, σ_z^2 are the mean and the variance of the amplitudes before integration.

Then the sample mean and the sample variance of the map cell at n th scan are respectively given by

$$\overline{X}(n) = \frac{1}{M}\sum_{j=1}^{M} X_j(n),\ S^2(n) = \frac{1}{M-1}\sum_{j=1}^{M}[X_j(n) - \overline{X}(n)]^2 \quad (3)$$

It is obtained from (3) that $\overline{X}(n)$ is a Gaussian variate, i.e. $\overline{X}(n) \sim N(m_R, \sigma_R^2/M)$, $(M-1)S^2(n)/\sigma_R^2$ is a chi square variate with $(M-1)$ degrees of freedom, i.e. $S^2(n) \sim \sigma_R^2(M-1)^{-1}\chi^2(M-1)$ and they are independent to each other [4].

Let us deal with the statistical characteristic of the outputs of the two loop integrators. The output $\overline{X}_f(n-1)$ of the upper loop integrator can be expressed as

$$\overline{X}_f(n-1) = (1-a)\sum_{l=0}^{n-1} a^l \overline{X}(n-1-l) \qquad (4)$$

Only considering the steady state of the clutter map procedure by letting $n \to \infty$, the mean and the variance of $\overline{X}_f(n-1)$ can be evaluated through (4) as

$$m_{\overline{X}_f} = m_R, \quad \sigma_{\overline{X}_f}^2 = \frac{1-a}{1+a}\cdot\frac{\sigma_R^2}{M} \qquad (5)$$

Since the PDF of $\overline{X}(n)$ is Gaussian, it can be acquired that $\overline{X}_f(n-1) \sim N(m_{\overline{X}_f}, \sigma_{\overline{X}_f}^2)$. The output $S_f^2(n-1)$ of the lower loop integrator can be expressed as

$$S_f^2(n-1) = (1-a)\sum_{l=0}^{n-1} a^l S^2(n-1-l) \qquad (6)$$

It is hard to determine the statistical distribution of the output $S_f^2(n-1)$ from (6). We recall $N_e = (1+a)/(1-a)$ as the effective length of the filter memory [5]. N_e can be considered as the number of equivalent pulses integrated by the clutter map. Thus $S_f^2(n-1)$ can be approximately expressed as

$$S_f^2(n-1) = \frac{1}{N_e}\sum_{i=0}^{N_e-1} S^2(n-1-i) \qquad (7)$$

Through the previous equation it can be predicted that the output $S_f^2(n-1) \sim \sigma_R^2(M-1)^{-1}N_e^{-1}\chi^2(N_e(M-1))$ [4]. To verify the conclusion, a chi square test has been carried out, using a population of 1000 samples of the lower loop integrator output. The test has been done for several

values of the map cell size M and the effective length N_e of the filter memory. It is shown that the hypothesis of chi square distribution can be admitted at a significance level of 5%, when $2 \le M \le 16$ and $N_e \ge 7$.

Next consider the statistic

$$\eta = \frac{[X_d(n) - \overline{X}_f(n-1)] \Big/ \sqrt{\sigma_R^2 + \sigma_{\overline{X}_f}^2}}{\sqrt{(M-1)N_e S_f^2(n-1) \big/ \sigma_R^2 \cdot 1/[(M-1)N_e]}} = \frac{X_d(n) - \overline{X}_f(n-1)}{\sqrt{1 + \frac{1}{MN_e}} S_f(n-1)} \quad (8)$$

Hence it is an ancillary statistic whose PDF is independent of m_z and σ_z^2. Under the hypothesis H_0 of no target situation, η is a Student-t variate with $N_e(M-1)$ degrees of freedom [4]. Letting T be the $(1-P_{fa})$ -quantile of η, we have the false alarm rate $P\{\eta > T \mid H_0\} = P_{fa}$ which is independent of m_z and σ_z^2. That proves the CFAR property of the GBCM-CFAR detector with some approximations. Thus the threshold coefficient is expressed as

$$H = \sqrt{1 + \frac{1}{MN_e}} T \quad (9)$$

3. PERFORMANCE ASSESSMENT

We now proceed to the performance of the GBCM-CFAR processor. The false alarm rate is given by

$$P_{fa} = P\{\eta > T \mid H_0\} = \int_T^\infty h_0(\eta) d\eta \quad (10)$$

where $h_0(\cdot)$ denotes the PDF of Student-t distribution with $N_e(M-1)$ degrees of freedom. If a nonfluctuating target exists in the background, the detection probability can be expressed as

$$P_d = P\{\eta > T \mid H_1\} = \int_T^\infty h_0[\eta - \frac{A_R}{\sigma_R}(1 + \frac{1}{N_e M})^{-1/2}] d\eta$$
$$= \int_T^\infty h_0[\eta - \lambda_R^{1/2}(1 + \frac{1}{N_e M})^{-1/2}] d\eta \quad (11)$$

where A_R denotes the signal amplitude after integration and $\lambda_R = A_R^2 / \sigma_R^2$ is the signal-to-clutter ratio (SCR) after integration. We introduce the SCR improvement factor (IF) employing R-pulse noncoherent integration [3]

$$IF = \frac{\lambda_R}{\lambda_z} = \frac{A_R^2 / \sigma_R^2}{A_z^2 / (m_z^2 + \sigma_z^2)} = \sqrt{R}(1 + \frac{m_z^2}{\sigma_z^2}) \quad (12)$$

where λ_z is the SCR before noncoherent integration. From (11) and (12) we may rewrite the expression for P_d related to the original SCR as

$$P_d = \int_T^\infty h_0[\eta - (IF \cdot \lambda_z)^{1/2}(1 + \frac{1}{N_e M})^{-1/2}] d\eta \quad (13)$$

Furthermore, with respect to the property that t-distribution is close to standard Gaussian distribution when the freedom degree is large [4], the performance of the GBCM-CFAR processor approaches the optimum Neyman-Pearson detector when $N_e \to \infty$, namely $a = 1$:

$$\lim_{N_e \to \infty} P_{fa} = 1 - \Phi(T) \quad (14)$$

$$\lim_{N_e \to \infty} P_d = 1 - \Phi(T - \sqrt{\lambda_R}) = 1 - \Phi[\Phi^{-1}(1 - P_{fa}) - \sqrt{IF \cdot \lambda_z}] \quad (15)$$

where $\Phi(\cdot)$ is the CDF of standard Gaussian distribution.

It is commonly accepted that the Weibull and lognormal distribution are suitable models to describe non-Rayleigh clutter. We apply the above theory to Weibull and lognormal clutter. The Weibull PDF is

$$f_w(x) = \frac{\beta}{\alpha}\left(\frac{x}{\alpha}\right)^{\beta-1} \exp\left[-\left(\frac{x}{\alpha}\right)^{\beta}\right] \quad x \ge 0, \alpha > 0, \beta > 0 \quad (16)$$

We acquire the IF of the Weibull distribution through (12)

$$IF_w = \sqrt{R} \frac{\Gamma(1 + 2/\beta)}{\Gamma(1 + 2/\beta) - [\Gamma(1 + 1/\beta)]^2} \quad (17)$$

The lognormal PDF is

$$f_l(x) = \frac{1}{x\sqrt{2\pi\beta^2}} \exp\left[-\frac{(\ln x - \alpha)^2}{2\beta^2}\right] \quad x \ge 0, \alpha \in R, \beta > 0 \quad (18)$$

Then the IF of the lognormal distribution is

$$IF_l = \sqrt{R} \frac{\exp(2\alpha + 2\beta^2)}{\exp(2\alpha + 2\beta^2) - \exp(2\alpha + \beta^2)} \quad (19)$$

In Fig. 3, curves of the threshold coefficient T required to achieve a false alarm rate of 10^{-6} for different map cell sizes M and for several values of N_e are shown. It reveals that as N_e or M increases lower values for the threshold coefficient are obtained in all cases, as expected. This suggests that as long as the assumption of local homogeneity holds true, the higher N_e and M, the better performance. This is consistent with the discussion leading to (14) and (15).

The results of the detection performance are presented in Fig. 4 for Weibull and lognormal background. Fig. 4(a) represents the detection performance versus the SCR λ_z before integration for $M = 8$, $R = 64$ and different values of N_e in Weibull clutter. In Fig. 4(a), the curves corresponding to the shape parameter $\beta = 1$ and $\beta = 2$ (i.e. the Rayleigh distribution as a special case of the Weibull distribution) are given, so as to elicit the influence of the clutter spikiness. All the plots refer to $P_{fa} = 10^{-6}$. For comparison purposes, the curves of the optimum Neyman-Pearson detector for both cases are also shown for the same value of P_{fa}. So the CFAR losses can be read from the figure as the horizontal displacement between the curve and the corresponding leftmost one. It is shown that the CFAR losses of both cases are below 1dB, namely that the performance of the GBCM-CFAR system is close to the optimal. Referring to the influence of the Weibull clutter shape parameter β on the detection performance,

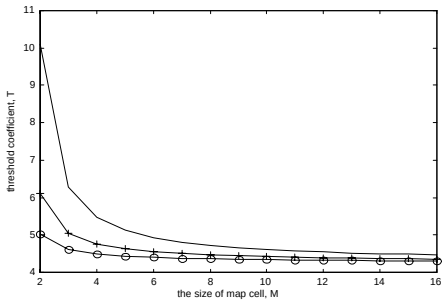

Figure 3: Threshold coefficient T versus M, the size of map cell, for different values of N_e, $P_{fa} = 10^{-6}$.

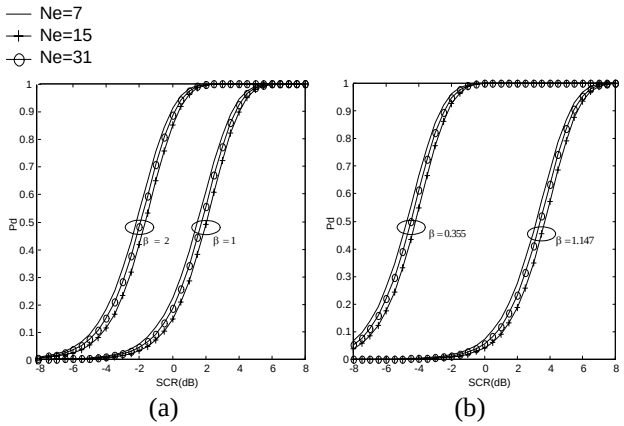

(a) (b)

Figure 4: Detection performance of GBCM-CFAR for point-like targets in Weibull and lognormal clutter. $M = 8$, $P_{fa} = 10^{-6}$, $R = 64$. (a) Weibull background, $\alpha = 0.9$, left: $\beta = 2$, right: $\beta = 1$. (b) lognormal background, $\alpha = 0.9$, left: $\beta = 0.355$, right: $\beta = 1.147$.

Ne=∞
Ne=15
Ne=31

it indicates that higher tails of the distribution result in worse performance. As to the detection probability of 0.9, the performance of $\beta = 1$ corresponding to the spikier clutter is shown about 4dB CFAR loss as to the case of $\beta = 2$.

Similar plots are depicted in Fig. 4(b) with reference to the case of lognormal clutter. The curves corresponding to the shape parameter $\beta = 0.355$ and $\beta = 1.147$ are given, because $\beta = 0.355$ makes the lognormal distribution as spiky as the Rayleigh one and the spikiness of the lognormal clutter with $\beta = 1.147$ is similar to the Weibull case with $\beta = 1$ [6]. The same conclusions are drawn as Weibull clutter for the CFAR loss and the heavy-tail effect. The CFAR loss between $\beta = 1.147$ and $\beta = 0.355$ of the lognormal clutter is larger than the Weibull case.

4. CONCLUSION

In this paper we have introduced and assessed a Gaussian biparametric clutter-map CFAR processor based on dividing the radar space into several map cells, in order to perform the background estimation. The CFAR property of the detector independent of the original clutter distribution has been proven with some approximations. The performance of the GBCM-CFAR procedure has been investigated subjective to Weibull and lognormal clutter with discussion of the effect of system parameters and distribution parameters. In the homogeneous environment, the performance of GBCM-CFAR is close to that of the optimum Neyman-Pearson detector with little CFAR losses as long as $N_e \geq 15$ and $M \geq 2$. It is also more suitable than GB-CFAR (or SW-CFAR) to cope with the nonhomogeneous situation.

However, GBCM-CFAR still suffers the masking effect. A possible solution is to enable or disable the update procedure of the loop integrator depending on whether or not a target is declared in the current scan. And further work should be done to analyze the sensitivity of the false alarm rate when the CFAR condition is not met, namely that there are some possible mismatches between the actual clutter condition and the detector design.

5. REFERENCES

[1] E. Conte, and M. Lops, "Clutter-map CFAR detection for range-spread targets in non-Gaussian clutter. Part I: System design", *IEEE Trans. Aerospace and Electronic Systems*, Vol. AES-33, pp. 432-443, April 1997.

[2] R. Nitzberg, "Clutter map CFAR analysis", *IEEE Trans. Aerospace and Electronic Systems*, Vol. AES-22, pp. 419-421, July 1986.

[3] H.D. Meng, X.Q. Wang, and Y.N. Peng, "New CFAR processor independent of original noise distribution", *Proceeding of CIE International Conference on Radar*, pp. 368-371, October 2001.

[4] J.K. Patel, C.H. Kapadia, and D.B. Owen, *Handbook of Statistical Distributions*, Marcel Dekker, New York, 1976.

[5] M. Lops, and M. Orsini, "Scan-by-scan averaging CFAR", *IEE Proc. F*, Vol. 136, pp.249-254, December 1989.

[6] E. Conte, M.D. Bisceglie, M. Lops, "Clutter-map CFAR detection for range-spread targets in non-Gaussian clutter. Part II: Performance assessment", *IEEE Trans. Aerospace and Electronic Systems*, Vol. AES-33, pp. 444-454, April 1997.